

Experimental verification of a modified fluctuation-dissipation relation for a micron-sized particle in a non-equilibrium steady state

Juan Ruben Gomez-Solano, Artyom Petrosyan, Sergio Ciliberto, Raphael Chetrite, Krzysztof Gawedzki

► To cite this version:

Juan Ruben Gomez-Solano, Artyom Petrosyan, Sergio Ciliberto, Raphael Chetrite, Krzysztof Gawedzki. Experimental verification of a modified fluctuation-dissipation relation for a micron-sized particle in a non-equilibrium steady state. *Physical Review Letters*, American Physical Society, 2009, 103 (4), pp.040601. 10.1103/PhysRevLett.103.040601 . ensl-00365952v3

HAL Id: ensl-00365952

<https://hal-ens-lyon.archives-ouvertes.fr/ensl-00365952v3>

Submitted on 23 Jun 2009

HAL is a multi-disciplinary open access archive for the deposit and dissemination of scientific research documents, whether they are published or not. The documents may come from teaching and research institutions in France or abroad, or from public or private research centers.

L'archive ouverte pluridisciplinaire **HAL**, est destinée au dépôt et à la diffusion de documents scientifiques de niveau recherche, publiés ou non, émanant des établissements d'enseignement et de recherche français ou étrangers, des laboratoires publics ou privés.

Experimental verification of a modified fluctuation-dissipation relation for a micron-sized particle in a non-equilibrium steady state

J. R. Gomez-Solano, A. Petrosyan, S. Ciliberto, R. Chetrite, and K. Gawędzki
*Université de Lyon, Laboratoire de Physique, Ecole Normale Supérieure de Lyon,
 CNRS, 46, Allée d'Italie, 69364 Lyon CEDEX 07, France*

A modified fluctuation-dissipation-theorem (MFDT) for a non-equilibrium steady state (NESS) is experimentally checked by studying the position fluctuations of a colloidal particle whose motion is confined in a toroidal optical trap. The NESS is generated by means of a rotating laser beam which exerts on the particle a sinusoidal conservative force plus a constant non-conservative one. The MFDT is shown to be perfectly verified by the experimental data. It can be interpreted as an equilibrium-like fluctuation-dissipation relation in the Lagrangian frame of the mean local velocity of the particle.

The validity of the fluctuation-dissipation theorem (FDT) in systems out of thermal equilibrium has been the subject of intensive study during the last years. We recall that for a system in equilibrium with a thermal bath at temperature T the FDT establishes a simple relation between the 2-time correlation function $C(t-s)$ of a given observable and the linear response function $R(t-s)$ of this observable to a weak external perturbation

$$\partial_s C(t-s) = k_B T R(t-s). \quad (1)$$

However, Eq. (1) is not necessarily fulfilled out of equilibrium and violations are observed in a variety of systems such as glassy materials [1, 2, 3, 4, 5], granular matter [6], and biophysical systems [7]. This motivated a theoretical work devoted to a search of a general framework describing FD relations, see the review [8] or [9, 10, 11, 12, 13, 14] for recent attempts in simple stochastic systems. In the same spirit, a modified fluctuation-dissipation theorem (MFDT) has been recently formulated for a non-equilibrium steady dynamics governed by the Langevin equation with non-conservative forces [15]. In particular, this MFDT holds for the overdamped motion of a particle on a circle, with angular position θ , in the presence of a periodic potential $H(\theta) = H(\theta + 2\pi)$ and a constant non-conservative force F

$$\dot{\theta} = -\partial_\theta H(\theta) + F + \zeta, \quad (2)$$

where ζ is a white noise term of mean $\langle \zeta_t \rangle = 0$ and covariance $\langle \zeta_t \zeta_s \rangle = 2D\delta(t-s)$, with D the (bare) diffusivity. This is a system that may exhibit an increase in the effective diffusivity [16, 17]. Here, we shall study the dynamical non-equilibrium steady state (NESS) reached for observables that depend only on the particle position on the circle so are periodic functions of the angle θ . Such a state corresponds to a constant non-vanishing probability current j along the circle and a periodic invariant probability density function $\rho_0(\theta)$ that allow us to define a mean local velocity $v_0(\theta) = j/\rho_0(\theta)$. This is the average velocity of the particle at θ . For a stochastic system in NESS evolving according to Eq. (2), the

MFDT reads for $t \geq s$

$$\partial_s C(t-s) - b(t-s) = k_B T R(t-s), \quad (3)$$

where the 2-time correlation of a given observable $O(\theta)$ is defined by

$$C(t-s) = \langle O(\theta_t) O(\theta_s) \rangle_0, \quad (4)$$

and the linear response function to a δ -perturbation of the conjugated variable h_t is given by the functional derivative

$$R(t-s) = \left. \frac{\delta}{\delta h_s} \right|_{h=0} \langle O(\theta_t) \rangle_h. \quad (5)$$

In Eq. (5), $\langle \dots \rangle_h$ denotes the average in the perturbed time-dependent state obtained from the NESS by replacing $H(\theta)$ in Eq. (2) by $H(\theta) - h_t O(\theta)$. It reduces for $h = 0$ to the NESS average $\langle \dots \rangle_0$. In Eq. (3), the correlation $b(t-s)$ is given by

$$b(t-s) = \langle O(\theta_t) v_0(\theta_s) \partial_\theta O(\theta_s) \rangle_0. \quad (6)$$

This new term takes into account the extent of the violation of the usual fluctuation-dissipation relation (1) due to the probability current and it plays the role of a corrective term to $C(t-s)$ in the MFDT, Eq. (3), which can be rewritten in the integral form:

$$C(0) - C(t) - B(t) = k_B T \chi(t), \quad (7)$$

where $B(t) \equiv \int_0^t b(t-s) ds$ and $\chi(t) = \int_0^t R(t-s) ds$ is the integrated response function.

In this letter, we present an experimental test of Eq. (7) in the linear response regime around a NESS attained by a micron-sized particle in a toroidal optical trap similar to the one used in [12]. We first show that the dynamics of the particle is well described by the Langevin equation (2) on a circle. Secondly, by measuring v_0 , $B(t)$, $C(t)$ and $\chi(t)$, we verify Eq. (7) for the observable $O(\theta) = \sin \theta$. The result can be interpreted as an equilibrium-like fluctuation-dissipation relation in the Lagrangian frame of the mean local velocity $v_0(\theta)$ [15]. We also check that $\rho_0(\theta)$ is frame invariant.

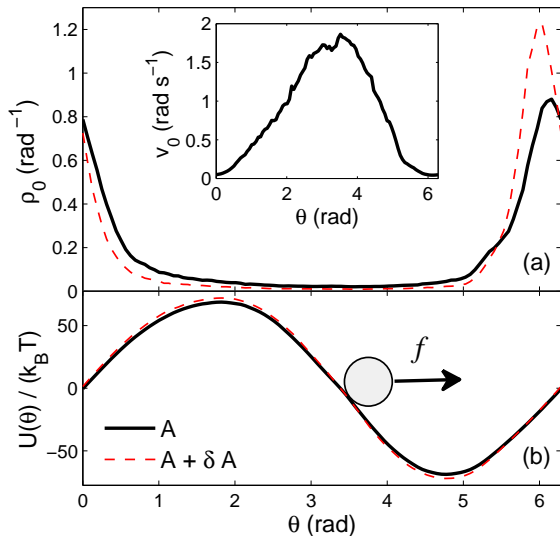


Figure 1: (a) Invariant density of the angular position of the particle in NESS for a modulation of 7% (black solid line) and 7.35% (red dashed line) around the laser mean power. Inset: Mean local velocity of the particle in the former case. (b) Corresponding potential profiles. The arrow indicates the direction of the non-conservative force f .

The experiment is performed using a spherical silica particle of radius $r = 1 \mu\text{m}$ in ultrapure water at room temperature $T = 20.0 \pm 0.5^\circ\text{C}$ at which the dynamic viscosity of water is $\eta = (1.002 \mp 0.010) \times 10^{-3} \text{ Pa s}$. The particle is kept by an optical tweezers in a toroidal optical trap. This kind of trap consists on a Nd:YAG diode pumped solid state laser beam ($\lambda = 1064 \text{ nm}$) which is focused by a microscope objective ($63\times$, $\text{NA} = 1.4$) and scans (by means of two acousto-optic deflectors) a circle of radius $a = 4.12 \mu\text{m}$ in the horizontal plane at a rotation frequency of 200 Hz. The toroidal trap is created 10 μm above the inner bottom surface of the cell where hydrodynamic boundary-coupling effects on the particle are negligible. At a rotation frequency of 200 Hz, the laser beam is not able to hold the particle but drags it regularly a small distance on the circle when passing through it [18]. The diffusive motion of the particle along the radial and vertical directions during the absence of the beam is less than 40 nm, thus the angular position of the particle θ (measured modulo 2π) is the only relevant degree of freedom of the dynamics. The laser power is sinusoidally modulated around 30 mW with an amplitude of 7% of the mean power, synchronously with the deflection of the beam at 200 Hz creating a static sinusoidal intensity profile along the circle. This trapping situation acts as a constant non-conservative force f associated to the mean kick which drives the particle across a sinusoidal potential $U(\theta)$ due to the periodic intensity profile. The particle barycenter (x_t, y_t) is measured by image analysis with an accuracy

of the order of 1 nm at a sampling rate of 150 Hz and exposure time of 1/300 s. This measure allows us to determine the angular position of the particle θ_t with respect to the trap center. For more details about the experimental apparatus see Ref. [19]. We determine the value of f and the profile of $U(\theta)$ by means of the method described in [20]. This method exploits the probability current j and the invariant density $\rho_0(\theta)$ in NESS to reconstruct the actual energy landscape of the particle. We recorded 200 time series $\{\theta_t\}$ of duration 66.67 s with different initial conditions $\{\theta_0\}$ sampled every 5 minutes in order to measure j and $\rho_0(\theta)$. The probability current is related to the global mean velocity of the particle by the expression $j = \langle \dot{\theta} \rangle_0 / (2\pi)$. The value of $\langle \dot{\theta} \rangle_0$ is calculated from the slope of the linear fit of the mean angular position of the particle (not taken modulo 2π) as a function of time leading to $j = 3.76 \times 10^{-2} \text{ s}^{-1}$ in the direction of the laser beam rotation. The invariant density, shown as a solid black line in Fig. 1(a), is computed from the histogram of each time series $\{\theta_t\}$ averaged over the 200 different initial conditions. In Fig. 1(a) we also show the mean local velocity $v_0(\theta) = j / \rho_0(\theta)$ of the particle. From these quantities we obtain $f = 3\eta r a j \int_0^{2\pi} \rho_0(\theta')^{-1} d\theta' = 6.60 \times 10^{-14} \text{ N}$ and $U(\theta) = -k_B T \log \rho_0(\theta) + \int_0^\theta (f - 6\pi\eta r a j \rho_0(\theta')^{-1}) a d\theta' = A \sin \theta$ with amplitude $A = 68.8 k_B T$. The experimental potential profile is shown in Fig. 1(b) (black solid line). Hence, the time evolution of θ is claimed to follow the Langevin dynamics of Eq. (2) [20] with $F = f / (6\pi\eta r a) = 0.85 \text{ rad s}^{-1}$, $H(\theta) = U(\theta) / (6\pi\eta r a^2) = H_0 \sin \theta$, $H_0 = A / (6\pi\eta r a^2) = 0.87 \text{ rad s}^{-1}$, and $D = k_B T / (6\pi\eta r a^2) = 1.26 \times 10^{-2} \text{ rad}^2 \text{ s}^{-1}$. Note that in the corresponding equilibrium situation ($f = 0$) the probability maximum would be located at the minimum of $U(\theta)$ ($\theta = 3\pi/2$). However, in NESS the non-conservative force $f > 0$ shifts the maximum of $\rho_0(\theta)$ in the positive direction, as shown in Fig. 1(a). The choice of the parameters has been done to enhance the stochastic nature of the dynamics, i.e. we take $(F - H_0) / H_0 \approx -2\%$ which is close to the maximum increase of the effective diffusivity following Refs. [16, 17].

Additionally, 500 times series of duration 100 s were specially devoted for the determination of $\chi(t)$. In this case, during each interval of 100 s we apply from time t_0 to $t_0 + \Delta t$ with $0 < t_0 < 66.67 \text{ s}$ and $\Delta t = 33.33 \text{ s}$ a step perturbation changing the value of A to $A + \delta A$. This is accomplished by suddenly switching the laser power modulation from 7% to 7.35% of the mean power (30 mW). The experimental value of the amplitude perturbation ($\delta A = 0.05A$) is determined from independent NESS measurements of $\rho_0(\theta)$ and $U(\theta)$ for a power modulation of 7.35% (shown in Figs. 1(a) and 1(b) respectively as red dashed lines) as described previously. By keeping constant the mean power during the switch we ensure that the value of f remains also constant, compare to a different time-dependent protocol explored re-

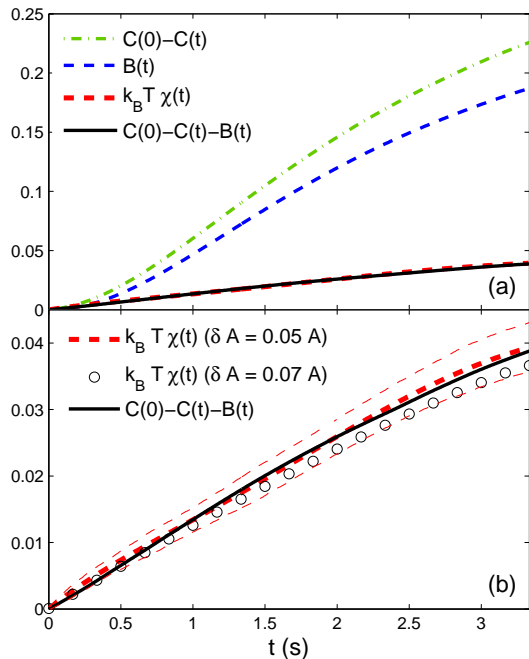


Figure 2: (a) Comparison between the different terms needed to verify Eq. (7), as functions of the time lag t . (b) Expanded view of the comparison between the curves $C(0) - C(t) - B(t)$ and $k_B T \chi(t)$ shown in Fig 2(a). The thin red dashed lines represent the error bars of the measurement of the integrated response.

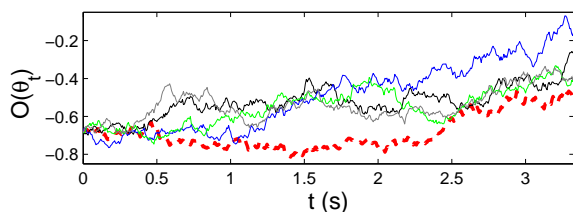


Figure 3: Example of trajectories used to compute the integrated response. We show a perturbed trajectory (thick dashed red line) and four out of a total of 200 of the corresponding unperturbed ones (see text).

cently in [21]. In this way, we extract 500 *perturbed* trajectories $\{\theta_t\}_{\delta A}$ of duration $\Delta t = 33.33$ s. We ensure that after switching off the perturbation the system actually has attained a NESS before the beginning of the next step perturbation.

With the purpose of determining correctly the different terms involved in Eq. (7), the observable $O(\theta)$ must be chosen consistently on both sides of such relation. The change of the potential $U(\theta) \rightarrow U(\theta) + \delta A \sin \theta$ due to the application of the step perturbation implies that $O(\theta) = \sin \theta$ is the observable that must be studied with $-\delta A$ as its conjugate variable. Hence, we compute the correlation function $C(t)$, the corrective term $B(t)$ (with $\partial_\theta O(\theta) = \cos \theta$ and the experimental curve $v_0(\theta)$ shown

in Fig. 1(a)) and the integrated response $\chi(t)$ for this observable, as functions of the time lag t .

The determination of $C(t)$ and $B(t)$ is straightforward according to Eqs. (4) and (6). The stationarity of the system allows us to perform an average over the time origin in addition to the ensemble average $\langle \dots \rangle_0$ over the 200 different time series devoted to this purpose, which increases enormously the statistics. The dependence of $C(0) - C(t)$ and $B(t)$ on t is shown in Fig. 2(a) in green dotted-dashed and blue dashed lines, respectively.

On the other hand, the integrated response $\chi(t)$ is given by

$$\chi(t) = \frac{\langle O(\theta_t) \rangle_{\delta A} - \langle O(\theta_t) \rangle_0}{-\delta A}. \quad (8)$$

In Eq. (8) the value $t = 0$ corresponds to instant t_0 when the perturbation of the potential amplitude δA is switched on. To decrease the statistical errors in comparison of the terms in Eq. (8), for a given perturbed trajectory $\theta_{t\delta A}$ we look for as many unperturbed ones θ_t as possible among the 200 time series $\{\theta_t\}$ starting at a time t^* such that $O(\theta_{t^*}) = O(\theta_{0\delta A})$. Then we redefine t^* as $t = 0$ in Eq. (8), as shown in Fig. 3. The unperturbed trajectories found in this way allow us to define a subensemble over which the average $\langle O(\theta_t) \rangle_0$ in Eq. (8) is computed at a given t . The average $\langle O(\theta_t) \rangle_{\delta A}$ is simply computed over the 500 perturbed time series. In Fig. 2(a) we show in thick dashed red line the dependence of the integrated response on t .

The comparison between the different terms needed to verify Eq. (3) is shown in Fig. 2(a), for the time lag interval $0 < t < 3.5$ s. As expected, the usual FD relation (1) is strongly violated in this NESS because of the broken detailed balance, with the correlation term $C(0) - C(t)$ being one order of magnitude larger than the response term $k_B T \chi(t)$. However, with the corrective term $B(t)$ associated to the probability current subtracted, $C(0) - C(t) - B(t)$ shown in solid black line in Fig. 2(a), becomes equal to $k_B T \chi(t)$. For clarity, in Fig. 2(b) we show an expanded view of the curves $C(0) - C(t) - B(t)$ and $k_B T \chi(t)$. We observe that, within the experimental error bars, the agreement between both terms is quite good, verifying the integrated form of the modified FD relation (7). The error bars of the integrated response curve at each time lag t are obtained from the standard deviation of the subensemble of unperturbed trajectories found for each perturbed trajectory, like the ones shown in thin solid lines in Fig. 3. We checked that the perturbation $\delta A = 0.05A$ is small enough to remain within the linear response regime. This is quantitatively seen in Fig. 2(b) where the response measured at $\delta A = 0.07A$ is represented by circles. We see that $\chi(t)$ is independent of δA within experimental errors showing that we are in the linear response regime. The MFDT is checked only for the first 3.5 s because after this time the evaluation of $\chi(t)$ is affected by large errors. Indeed during the measure-

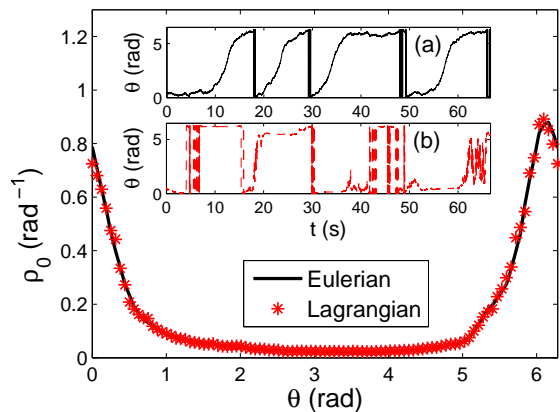


Figure 4: Invariant density of the angular position measured in the Eulerian frame (continuous line) (same as in Fig. 1(a)) and in the Lagrangian frame (*). Inset : example of a trajectory measured respectively in the Eulerian (a) and Lagrangian (b) frames.

ment of $\chi(t)$, for finite δA the system is approaching a new NESS which depends non-linearly on δA (see the strong non-linear dependence of ρ_0 on δA in Fig. 1(a)). The perturbed trajectories diverge with respect to the unperturbed ones (Fig. 3) in such a way that after 3.5 s the non-linear effects and the statistical error bars of $\chi(t)$ due to finite sampling become large.

As shown in [15], the validity of Eq. (7) for the fluctuations of the angular position of the silica particle in NESS gains a simpler interpretation in the Lagrangian frame of the mean local velocity $v_0(\theta)$ along the circle.

Indeed, using the observables that are time indepen-

dent in the Lagrangian frame, the MFDT may be rewritten in the form

$$\partial_s C_L(t, s) = k_B T R_L(t, s), \quad (9)$$

where C_L and R_L are the correlation and the response measured in the Lagrangian frame. Eq. (9) is close to that of the equilibrium FDT (Eq. (1)) except for the lack of the time translation invariance of the functions involved. One of the new predictions of the Lagrangian analysis of the system is that, although the trajectories in the Eulerian and the Lagrangian frame are quite different, their average density ρ_0 is the same in the two frames. This property is clearly illustrated by the experimental data in Fig. 4, where we compare the densities measured in the two frames. The insets of Fig. 4 point out to the difference between a trajectory measured in the Eulerian frame and the same trajectory measured in the Lagrangian frame.

We have verified experimentally a modified fluctuation-dissipation relation describing the dynamics of a system with one degree of freedom in NESS, namely a Brownian particle moving in a toroidal optical trap. We point out that the experimental results reported here represent an alternative approach to non-equilibrium fluctuation-dissipation relations to that of Ref. [12] which dealt with the velocity fluctuations relative to the mean local velocity. The approach followed in our work relies on an observable depending on the particle position. It quantifies the extent of the violation of the usual FDT by means of the term $B(t)$, admitting a transparent Lagrangian interpretation of the resulting MFDT.

-
- [1] L. F. Cugliandolo, J. Kurchan, and L. Peliti, Phys. Rev. E **55**, 3898 (1997).
 - [2] T. S. Grigera and N. E. Israeloff, Phys. Rev. Lett., **83**, 5038 (1999); L. Bellon, S. Ciliberto, and C. Laroche, Europhys. Lett., **53** (4), 511 (2001); D. Herisson and M. Ocio, Phys. Rev. Lett. **88**, 257202 (2002); L. Buisson and S. Ciliberto, Physica D, **204** (1-2) 1 (2005).
 - [3] L. Berthier and J.-L. Barrat, Phys. Rev. Lett. **89**, 095702 (2002).
 - [4] A. Crisanti and F. Ritort, J. Phys. A **36**, R181 (2003).
 - [5] P. Calabrese and A. Gambassi, J. Phys. A **38**, R133 (2005).
 - [6] A. Barrat, V. Colizza, and V. Loreto, Phys. Rev. E **66**, 011310 (2002).
 - [7] K. Hayashi and M. Takano, Biophys. J. **93**, 895 (2007).
 - [8] U. Marini Bettolo Marconi, A. Puglisi, L. Rondoni and A. Vulpiani, Physics Reports **461**, 111 (2008).
 - [9] K. Hayashi and S. I. Sasa, Phys. Rev. E **69**, 066119 (2004).
 - [10] T. Harada and S. I. Sasa, Phys. Rev. Lett. **95**, 130602 (2005).
 - [11] T. Speck and U. Seifert, Europhys. Lett. **74**, 391 (2006).
 - [12] V. Blickle, T. Speck, C. Lutz, U. Seifert, and C. Bechinger, Phys. Rev. Lett. **98**, 210601 (2007).
 - [13] T. Sakaue and T. Ohta, Phys. Rev. E **77**, 050102(R) (2008).
 - [14] M. Baiesi, C. Maes, and B. Wynants, arXiv:0902.3955v1 [cond-mat.stat-mech]
 - [15] R. Chetrite, G. Falkovich, and K. Gawedzki, J. Stat. Mech. P08005 (2008).
 - [16] P. Reimann, C. Van den Broeck, H. Linke, P. Hänggi, J. M. Rubi, and A. Pérez-Madrid, Phys. Rev. Lett. **87**, 010602 (2001).
 - [17] S.-H. Lee, and D. G. Grier, Phys. Rev. Lett. **96**, 190601 (2006).
 - [18] L. P. Faucheux, G. Stolovitzky, and A. Libchaber, Phys. Rev. E **51**, 5239 (1995).
 - [19] P. Jop, J. R. Gomez-Solano, A. Petrosyan, and S. Ciliberto, J. Stat. Mech. P04012 (2009).
 - [20] V. Blickle, T. Speck, U. Seifert, and C. Bechinger, Phys. Rev. E **75**, 060101(R) (2007).
 - [21] V. Blickle, J. Mehl, and C. Bechinger, arXiv:0902.2650v1 [cond-mat.soft].